PNAS
www.pnas.org

Supplementary Information for

Structures of ABCB4 provide insight into phosphatidylcholine translocation

Kamil Nosol, Rose Bang-Sørensen, Rossitza N. Irobalieva, Satchal K. Erramilli, Bruno Stieger, Anthony A. Kossiakoff, Kaspar P. Locher[1]

[1]Correspondence to be addressed to: locher@mol.biol.ethz.ch

This PDF file includes:

Figures S1 to S10
Table S1

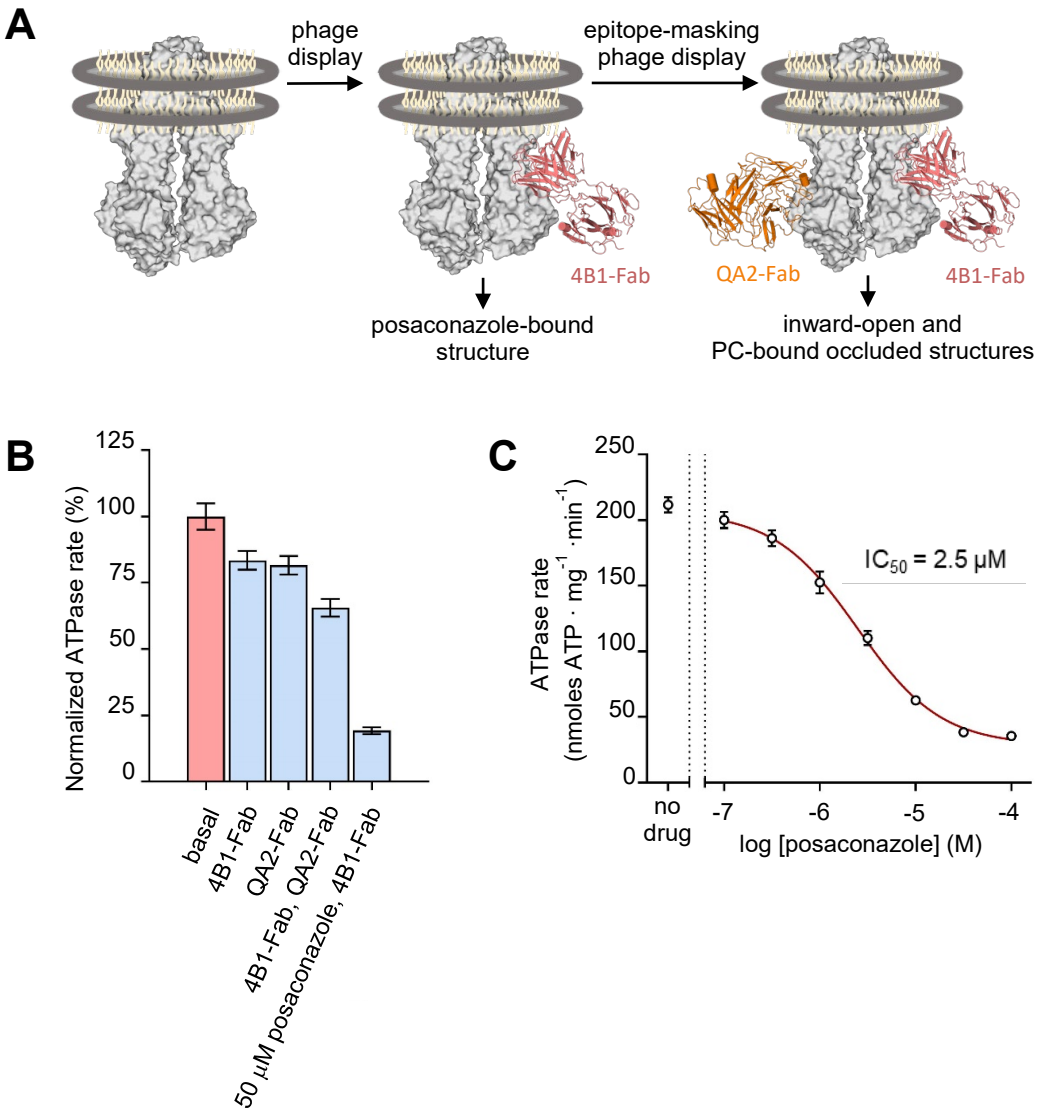

Fig. S1. Conformation-specific Fab fragments against ABCB4 and functional analysis.

(**A**) Strategy employed for selecting conformation-specific Fab fragments against ABCB4. Two consecutive steps of phage display were employed. First, nanodisc-reconstituted ABCB4 was used to select a binder termed 4B1-Fab, which bound the C-terminal half of the transporter. In a second strategy, the complex ABCB4:4B1-Fab was used as a target. Because 4B1-Fab masked the immunodominant epitope, we could isolate a binder specific to the N-terminal half of ABCB4, termed QA2-Fab. The grey surface shows ABCB4, the rings and lipids depict the nanodisc structure. (**B**) Normalized ATP hydrolysis rates of nanodisc-reconstituted ABCB4 in the absence or presence of Fabs. The ATPase activity of ABCB4 was reduced by ~20% when bound to one of the Fabs and by ~40% when bound to both. Each bar represents the mean of three independent measurements and error bars indicate SDs. (**C**) ATPase rate of nanodisc-reconstituted ABCB4 at varying posaconazole concentrations. Posaconazole reduces the rate to ~15% with an IC_{50} value of 2.5 µM (95% confidence interval, 2.08 µM – 2.96 µM) consistent with previous reports (5). Data represent the mean ± SD of three independent experiments.

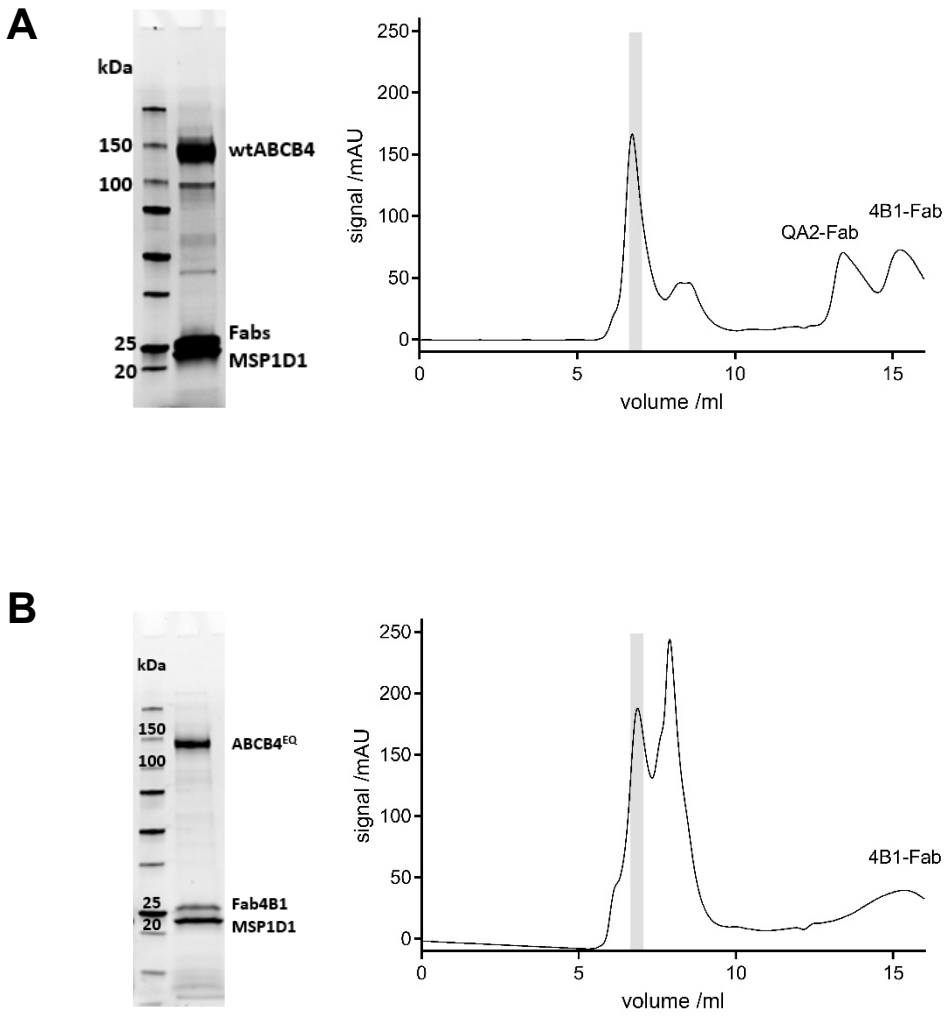

Fig. S2. Preparation of ABCB4-Fab complexes for cryo-EM analysis.
(**A-B**) SDS-PAGE analysis (left) and size exclusion chromatography of purified samples of ABCB4 reconstituted in nanodiscs as prepared for cryo-EM data collection. (**A**) Wild type ABCB4 in a complex with 4B1-Fab and QA2-Fab. (**B**) $ABCB4_{EQ}$ in a complex with 4B1-Fab. Grey areas depict pooled fractions used for grid preparation.

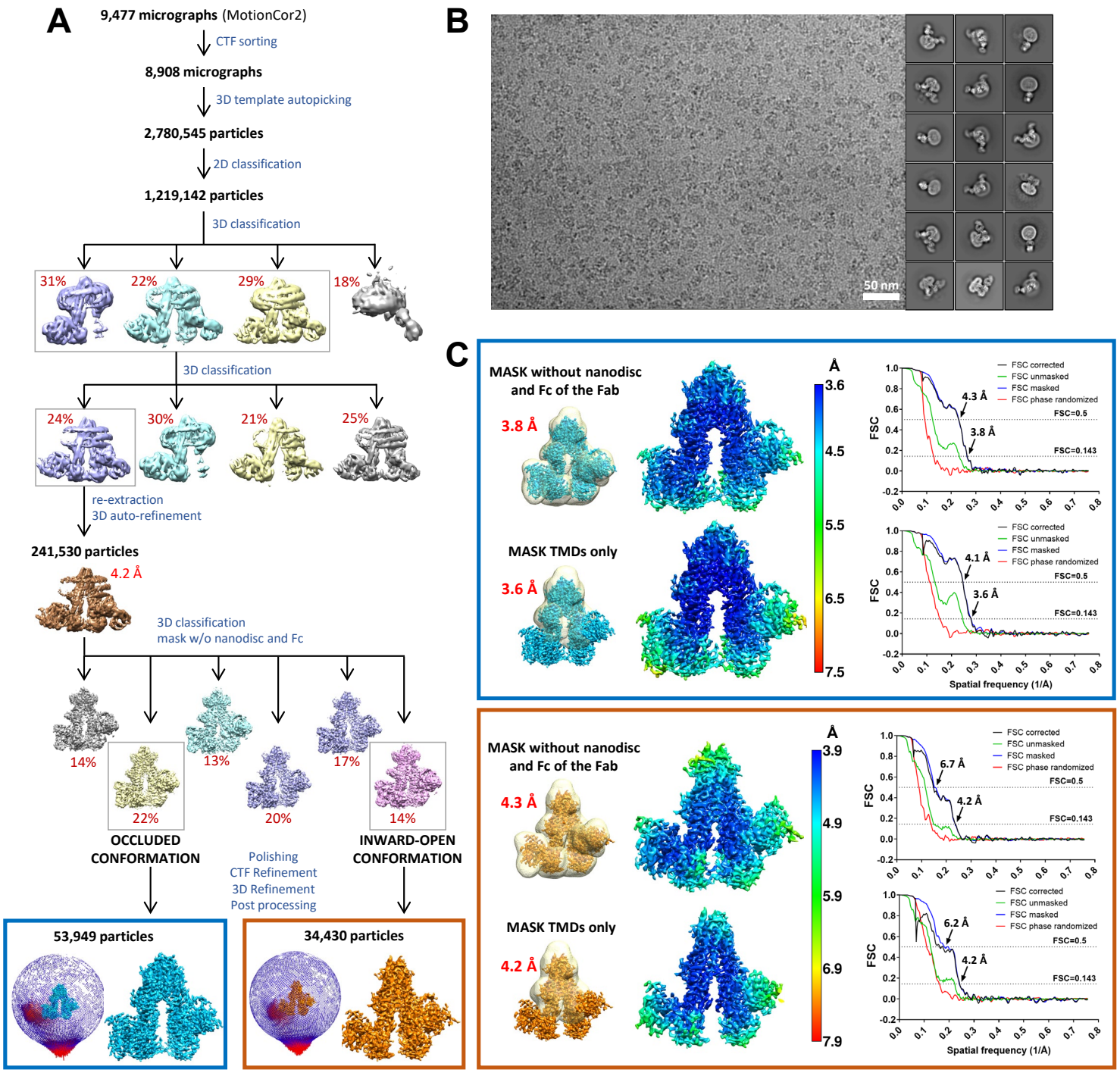

Fig. S3. Cryo-EM analysis of the wild-type ABCB4:(4B1-Fab):(QA2-Fab) complex.
(**A**) Flowchart of data processing using RELION 3.1 including angular distribution of the particles in the final classes. (**B**) Representative micrograph and 2D class averages. (**C**) Local resolution estimates of the final EM density maps and the corresponding FSC curves, calculated in RELION 3.1.

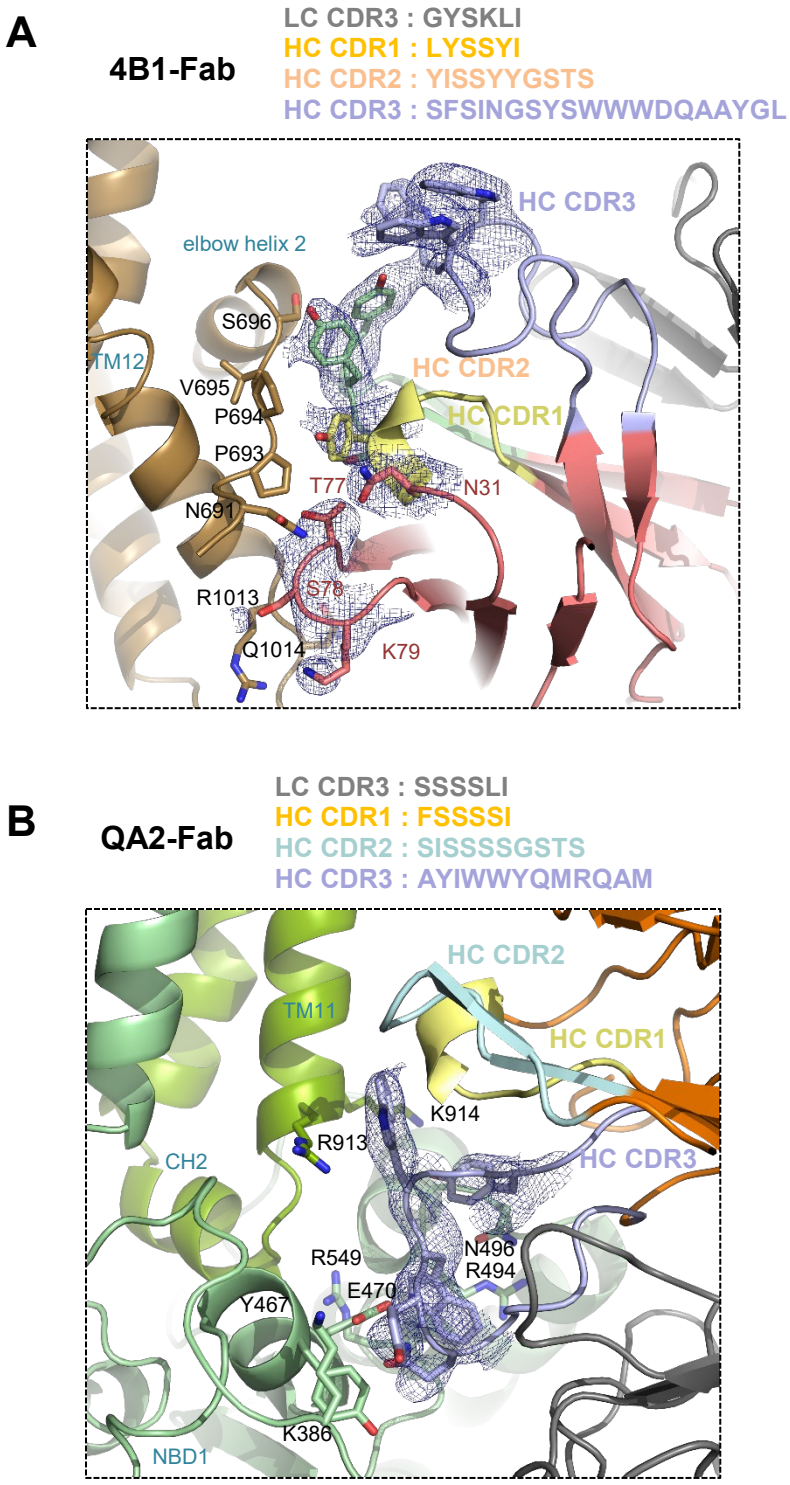

Fig. S4. ABCB4-Fab interfaces.
Close-up view of the ABCB4 binding epitopes for 4B1-Fab (**A**) and QA2-Fab (**B**). 4B1-Fab binds to the elbow helix of TMD2 (preceding TM7) as well as the linker between TM12 and the second nucleotide binding domain (NBD2), whereas QA2-Fab binds to TM11 and NBD1. ABCB4 is colored brown and green as in Figs. 1 and 2. Residues involved in the protein-protein interface are represented as sticks. The complementarity-determining regions (CDRs) are individually colored and labeled.

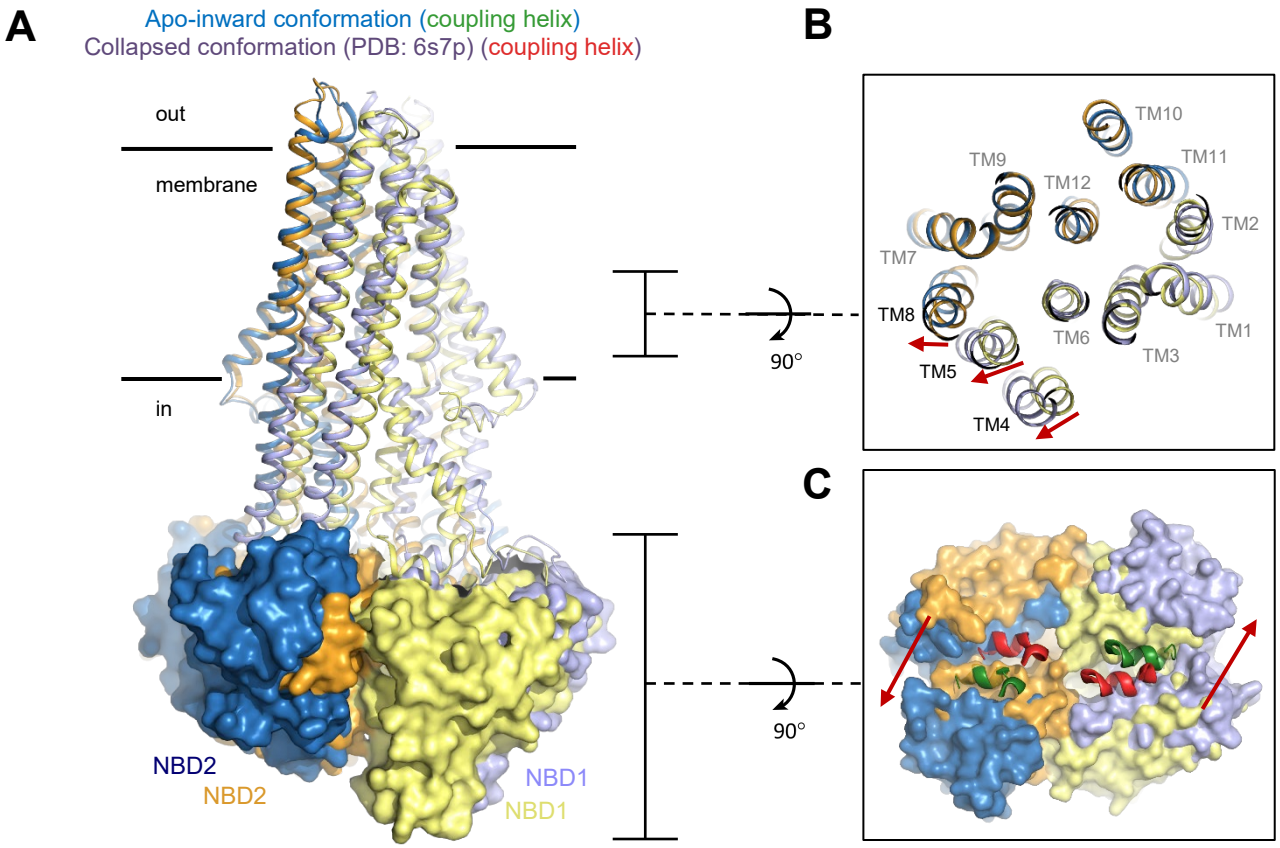

Fig. S5. Comparison between ABCB4 in apo-inward and closed conformation.
(**A**) Ribbon diagram (NBDs as surface) of apo-inward conformation of ABCB4 (dark and light blue) superimposed with the structure of ATP-bound $ABCB4_{EQ}$ in the closed conformation (yellow and orange, PDB ID 6S7P)(12), using the TMDs as an anchor for the superposition. (**B**) Horizontal slice shows the conformational changes in the TMDs. TM helices are shown as ribbons and labeled, red arrows show shifts in TM helix position. (**C**) View onto the NBDs from the membrane. Coupling helices are shown in green for the apo-inward conformation and in red for the ATP-bound state. Red arrows indicate the direction of the shift of the NBDs.

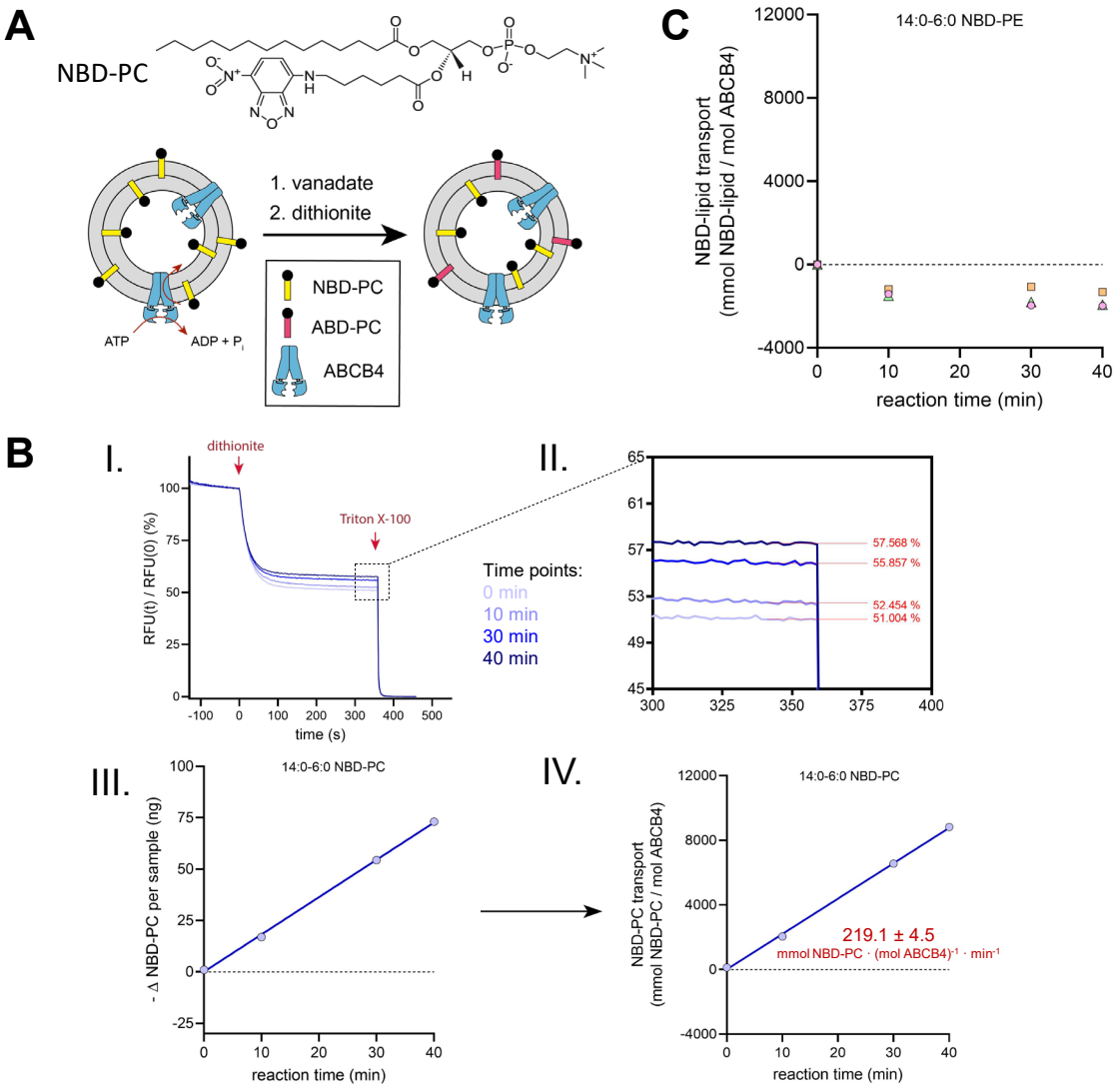

Fig. S6. ABCB4-mediated PC translocation assays.
(**A**) Representative structure of 14:0-6:0 NBD-PC. Schematic of proteoliposome-based *in vitro* assay of ABCB4 using fluorescently labeled phospholipids. The NBD fluorophore, attached to the lipid alkyl chain, can be reduced to a non-fluorescent product (ABD) by the reducing agent dithionite. (**B**) Primary measurements of the proteoliposome-based PC translocation assay. Shown are the results of a representative reaction sample (0.3% 14:0-6:0 NBD-PC). Each reaction was initiated by addition of 4 mM ATP and 10 mM Mg^{2+} and measured over the course of 40 minutes. At specific time points, samples were collected and mixed with vanadate to stop the ABCB4-catalyzed reaction. Next, dithionite was added to each sample and the decrease in fluorescence due to the reduction of the accessible fluorophore was recorded (I). The resulting fluorescence was averaged over 20 s (II). Data were normalized and plotted showing the percentage of translocated NBD-PC (light color spectrum corresponds to the time point of 0 min and dark color spectrum 40 min). Next, the differences in fluorescence quenching were plotted against the reaction time of the translocation reaction (III). The values were then converted to the number of NBD-PC molecules translocated (IV). To do so, the orientation of the protein was assumed to be 50:50 inside-out and right-side-out. The slope of the linear regression indicated the transport rate. (**C**) Result of an assay using fluorescently labeled PE instead of PC. Proteoliposomes were formed from a mixture of liver polar lipids and cholesterol (4:1 wt/wt) supplemented with 0.3% of 14:0-6:0 NBD-PE. Measurements were performed in triplicates and no specific kinetic analysis was performed.

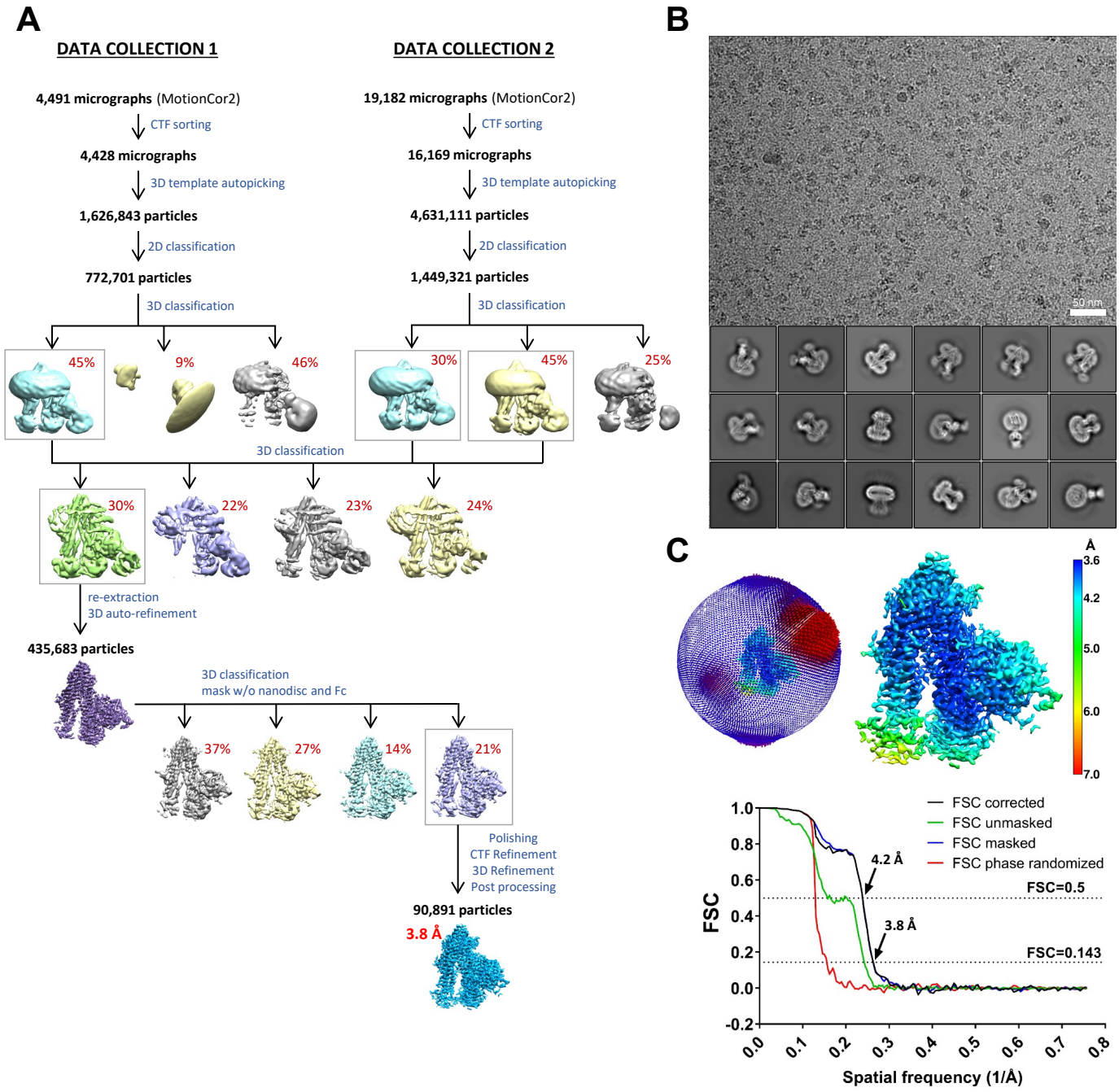

Fig. S7. Cryo-EM analysis of posaconazole-bound ABCB4$_{EQ}$:4B1-Fab complex.
(**A**) Flowchart of data processing using RELION 3.1. (**B**) Representative micrograph and 2D class averages. (**C**) Angular distribution of the particles in the final class, local resolution estimation of the final EM maps and corresponding FSC curves, calculated in RELION 3.1.

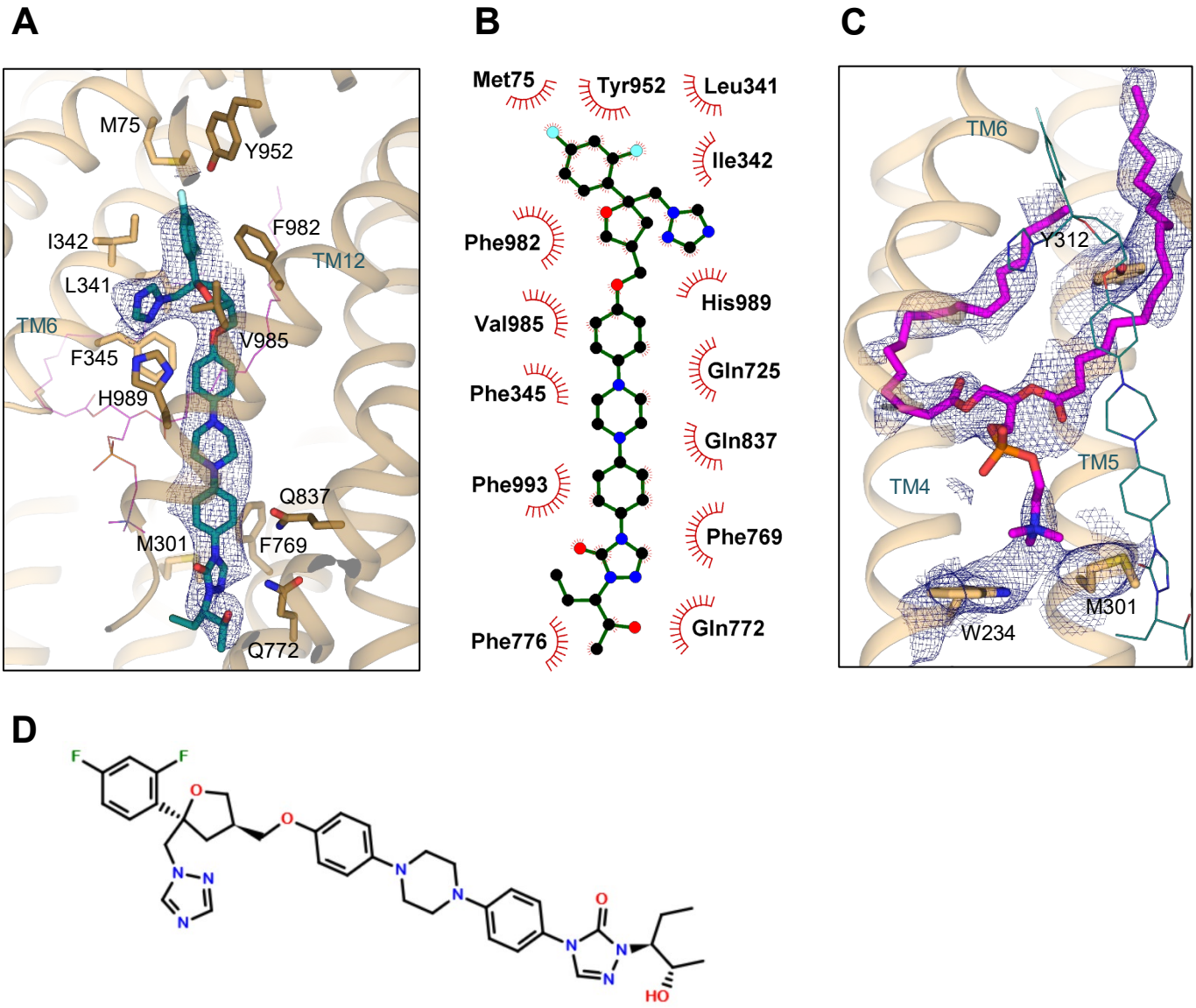

Fig. S8. Ligand interactions in posaconazole-bound ABCB4 structure.
(**A**) Close-up view of the binding pocket. Bound posaconazole is shown as sticks with carbons in green. Side chains of residues within 3.5 Å of bound posaconazole molecule are shown as sticks and labeled. The EM density of posaconazole is shown as a blue mesh. (**B**) Roadkill plot of bound posaconazole. (**C**) Close-up view of the side opening showing bound phospholipid in purple sticks. Side chains of selected residues are shown as sticks, EM density around bound PC is shown as a blue mesh. (**D**) Chemical structure of posaconazole molecule.

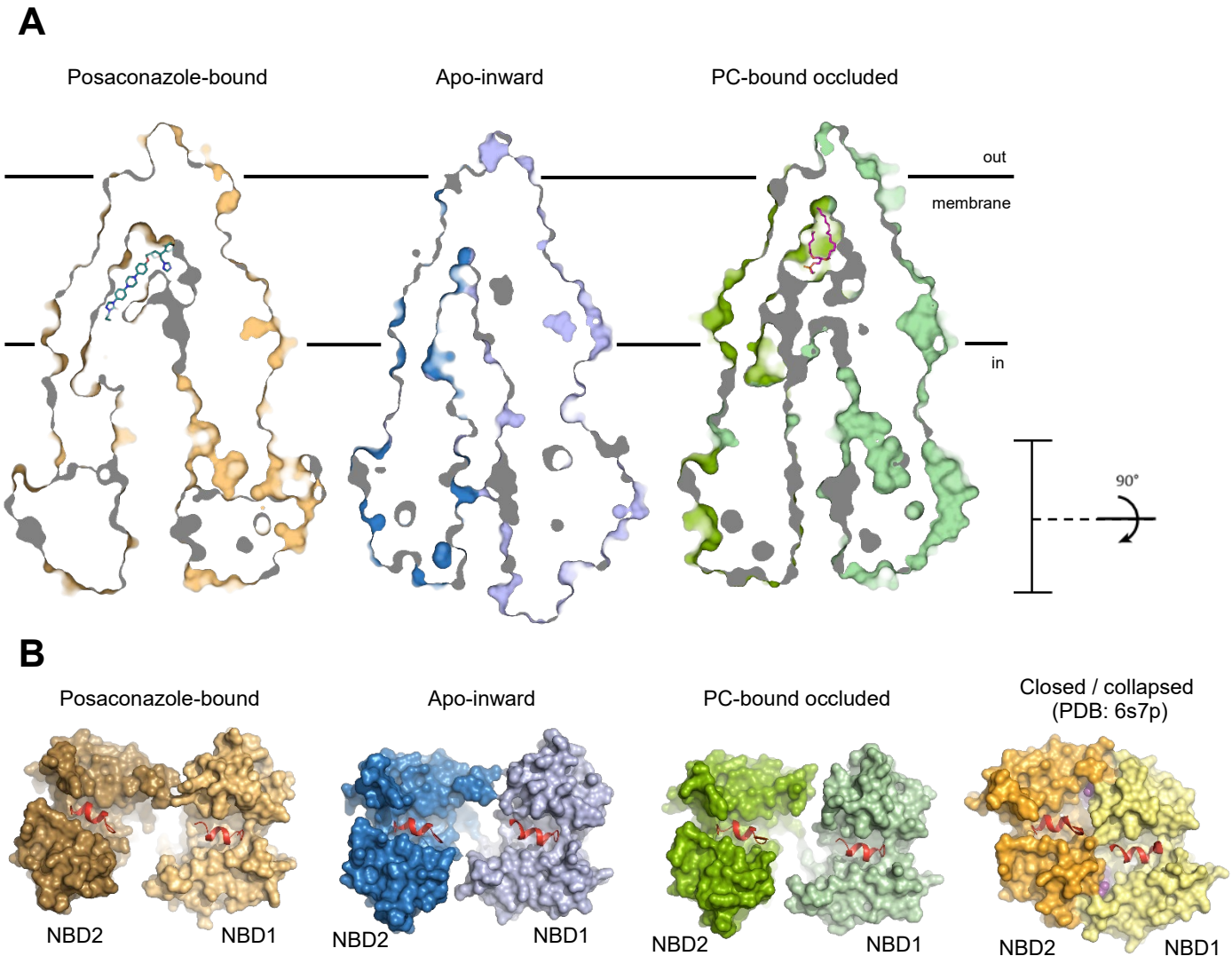

Fig. S9. Conformational changes of ABCB4 during the transport cycle.
(**A**) Vertical slice through a surface representation of posaconazole-bound, apo-inward and PC-bound conformations of ABCB4. The lipid and inhibitor molecules are represented as sticks. The black bracket indicates the view presented in panel B. (**B**) Surface representation of NBDs of available ABCB4 structures. The coupling helices interacting with the NBDs are shown as red ribbons.

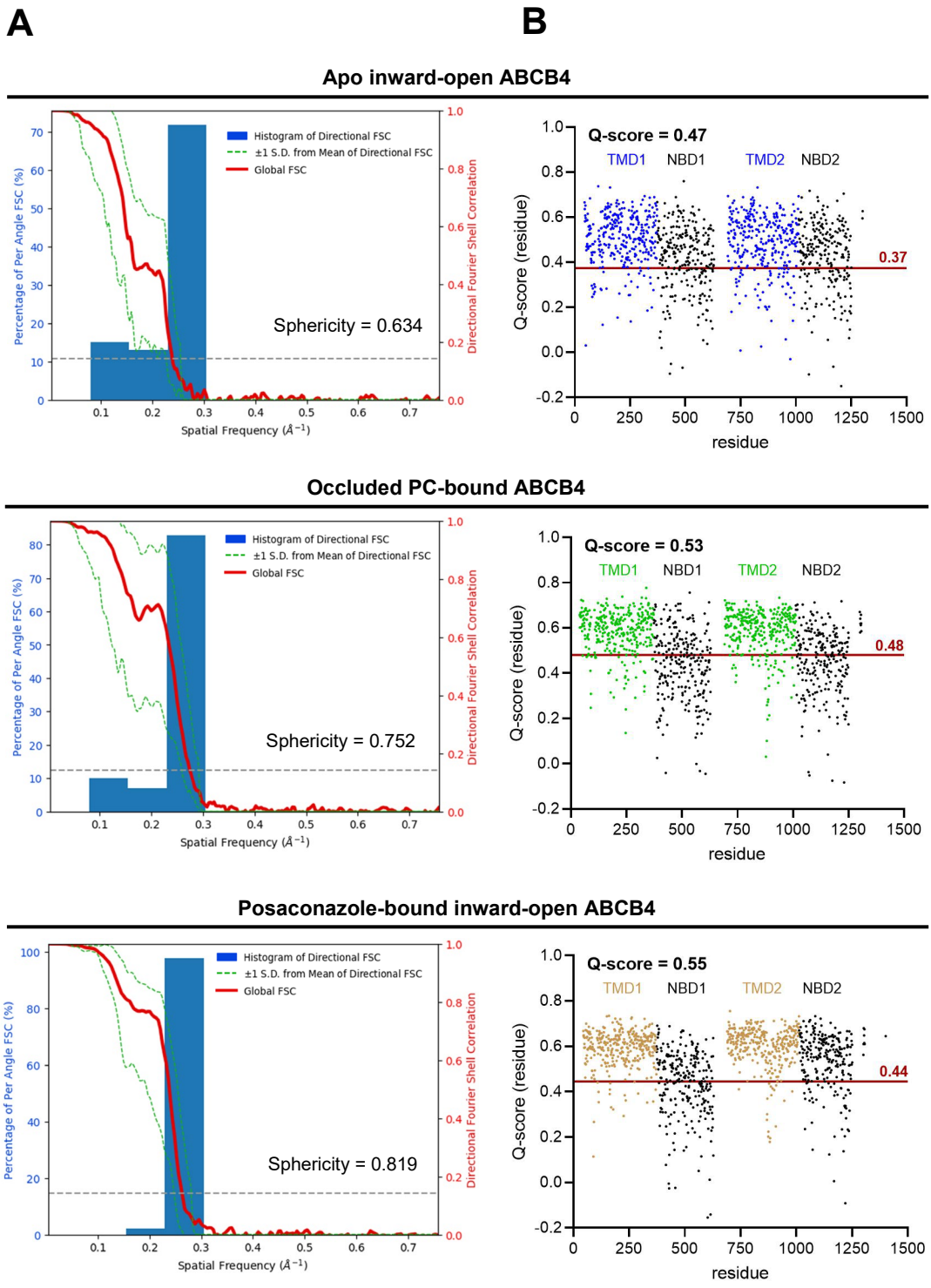

Fig. S10. 3DFSC and Q-score plots of the three ABCB4 structures.
(**A**) Histogram and directional FSC plot for ABCB4 (with Fc masked out) in three distinct conformations generated on the remote 3DFSC processing server. Sphericity values are indicated. (**B**) Per-residue Q-scores for each structure with TMD1/2 and NBD1/2 indicated in different colors (the Fab residues were excluded). The average Q-score for each structure is indicated on each plot. The red line and value indicate the expected Q-score based on the calculated resolution of each map (as per the 0.143 criterion).

Table S1. Cryo-EM data collection, refinement and validation statistics.

	apo-inward **wtABCB4**:4B1-Fab:QA2-Fab (EMDB-**12365**) (PDB **7NIU**)	**PC-bound occluded** **wtABCB4**:4B1-Fab:QA2-Fab (EMDB-**12366**) (PDB **7NIV**)	**posaconazole-bound** **ABCB4$_{EQ}$**:4B1-Fab (EMDB-**12367**) (PDB **7NIW**)
Data collection and processing			
Magnification	130,000	130,000	130,000
Voltage (kV)	300	300	300
Electron exposure (e^{-}/Å^2)	80.4	80.4	68.5
Exposure time (s)	1.2	1.2	1.2
Number of frames per movie	40	40	40
Defocus range (μm)	-0.6 – -2.2	-0.6 – -2.2	-0.6 – -2.2
Pixel size (Å)	0.66	0.66	0.66
Number of movies	9,477	9,477	23,673
Symmetry imposed	C1	C1	C1
Initial particle number	2,780,545	2,780,545	6,257,954
Final particle number	34,430	53,949	90,891
Map resolution (Å)	4.2	3.6	3.8
FSC threshold	0.143	0.143	0.143
Map resolution range (Å)	4.02 – 8.72	3.56 – 7.99	3.66 – 8.10
Refinement			
Initial model used (PDB code)	6S7P / 6UKJ	6S7P / 6UKJ	6S7P / 6UKJ
Map sharpening *B* factor (Å^2)	-100	-84	-104
Model composition			
Non-hydrogen atoms	15,507	15,736	12,483
Protein residues	2,015	2,020	1,585
Ligands (CLR – cholesterol)	0 (2 CLR)	1 (7 CLR)	2 (6 CLR)
B factors (Å^2)			
Protein	50.89	29.30	80.01
Ligand	30.00	6.97	42.71
R.m.s. deviations			
Bond lengths (Å)	0.008	0.007	0.015
Bond angles (°)	0.998	0.968	1.221
Validation			
MolProbity score	2.68	2.37	2.73
Clashscore	29.35	21.68	25.33
Poor rotamers (%)	1.25	0.65	1.68
Ramachandran plot			
Favored (%)	85.19	90.45	84.38
Allowed (%)	14.71	9.50	15.49
Disallowed (%)	0.10	0.05	0.13